Human iPSC-derived Committed Cardiac Progenitors Generate Cardiac Tissue Grafts in a Swine Ischemic Cardiomyopathy Model without Triggering Ventricular Arrhythmias

Amish N. Raval MD[1,2]*, Eric G. Schmuck PhD[1], Sushmita Roy PhD[1], Yukihiro Saito MD, PhD[1], Tianhua Zhou MD[1], James Conklin[2], Timothy A. Hacker PhD[3], Chad Koonce[4], Meghan Boyer[4], Kristin Stack[4], Ellen Hebron[4], Scott K. Nagle MD, PhD[5], Patrick C.H. Hsieh MD, PhD[1,6,7], Timothy J. Kamp MD, PhD[1,6]*

[1]Department of Medicine, Division of Cardiovascular Medicine, University of Wisconsin School of Medicine and Public Health, Madison, WI, USA.

[2]Department of Biomedical Engineering, University of Wisconsin, Madison, USA

[3]Cardiovascular Research Center, University of Wisconsin-Madison School of Medicine and Public Health, Madison, USA

[4]Fujifilm Cellular Dynamics Inc., Madison, WI, USA

[5]Department of Radiology, University of Wisconsin School of Medicine and Public Health, Madison, WI, USA

[6]Department of Cell and Regenerative Biology, University of Wisconsin-Madison, USA

[7]Institute of Biomedical Sciences, Academia Sinica, Taipei, Taiwan.

*To whom correspondence should be addressed:

Timothy J. Kamp, tjk@medicine.wisc.edu, 1111 Highland Ave., WIMR II 8459, Madison, WI 53705

Amish N Raval, anr@medicine.wisc.edu, H4/568, Box 3248 Clinical Science Center, 600 Highland Ave., Madison, WI 53792

Short Title: Committed Cardiac Progenitors for Cardiac Repair

Journal Subject Terms: Cell Therapy, Stem cells, Heart Failure, Chronic Ischemic Heart Disease, Treatment.

ABSTRACT

Background: The adult human heart following a large myocardial infarction is unable to regenerate heart muscle and instead forms scar with the risk of progressive heart failure. Large animal studies have shown that intramyocardial injection of human pluripotent stem cell-derived cardiomyocytes (hPSC-CMs) following a myocardial infarction result in cell grafts but also ventricular arrhythmias. We hypothesized that intramyocardial injection of committed cardiac progenitor cells (CCPs) derived from iPSCs, combined with cardiac fibroblast-derived extracellular matrix (cECM) to enhance cell retention will: i) form cardiomyocyte containing functional grafts, ii) be free of ventricular arrhythmias and iii) restore left ventricular contractility in a post-myocardial infarction (MI) cardiomyopathy swine model.

Methods: hiPSCs were differentiated using bioreactors and small molecules to produce a population of committed cardiac progenitor cells (CCPs). MI was created using a coronary artery balloon occlusion and reperfusion model in Yucatan mini pigs. Four weeks later, epicardial needle injections of CCPs+cECM were performed in a small initial feasibility cohort, and then transendocardial injections (TEI) of CCPs+cECM, CCPs alone, cECM alone or vehicle control into the peri-infarct region in a larger randomized cohort. A 4-drug immunosuppression regimen was administered to prevent rejection of human CCPs. Arrhythmias were evaluated using implanted event recorders. Magnetic resonance imaging (MRI) and invasive pressure volume assessment were used to evaluate left ventricular anatomic and functional performance, including viability. Detailed histology was performed on the heart to detect human grafts.

Results: A scalable biomanufacturing protocol was developed generating CCPs which can efficiently differentiate to cardiomyocytes or endothelial cells in vitro. Intramyocardial delivery of CCPs to post-MI porcine hearts resulted in engraftment and differentiation of CCPs to form ventricular cardiomyocyte rich grafts. There was no significant difference in cardiac MRI-based measured cardiac volumes or function between control, CCP and CCP+cECM groups; however, dobutamine stimulated functional reserve was improved in CCP and CCP+cECM groups. TEI delivery of CCPs with or without cECM did not result in tumors or trigger ventricular arrhythmias.

Conclusions: CCPs are a promising cell source for post-MI heart repair using clinically relevant TEI with a low risk of engraftment ventricular arrhythmias.

Key words: Stem Cell, Heart Failure, Treatment, Trial, Catheter

INTRODUCTION

Currently approved medication and device therapies can blunt the progression of heart failure (HF) following myocardial infarction (MI), but the morbidity and mortality in post - MI survivors remain significant.[1, 2] For patients who suffer large MIs, replacement of necrotic myocardium with fibrotic scar frequently leads to progressive heart failure, and there are currently no available treatments to replace lost cardiomyocytes and restore contractility. Therefore, cell-based therapies have been investigated for their potential to generate functional cardiac tissue in post-MI or ischemic cardiomyopathy animal models and patients. More than two decades of investigations and clinical trials with a variety of adult cell sources such as bone marrow mononuclear cells have produced no clear evidence of new functional heart muscle or consistent improvements in clinical outcomes.[3] In contrast, post-MI delivery of human pluripotent stem cell (PSC)-derived cardiomyocytes (CMs) from embryonic stem cells (ESCs) or induced pluripotent stem cells (iPSCs) has produced viable cardiomyocyte grafts in rat,[4-6] guinea pig,[7-9] swine,[10, 11] and non-human primate[12-14] myocardium. However, large animal experimental studies using hPSC-CMs have been complicated by ventricular arrhythmias, relatively low cell retention in the myocardium and mixed functional results.

hPSC-derived cardiac progenitor cells are also being investigated for cardiac cell therapy in the post-MI failing heart,[15, 16] but progenitor cells are a less studied cell preparation for therapy relative to hPSC-CMs. However, there are several features that make cardiac progenitors cells a promising cell source. Cardiac progenitor cells are smaller cells than hPSC-CMs and more amenable to manipulation and cell delivery while maintaining viability. The hPSC-derived cardiac progenitor cells are proliferative and can generate larger hPSC-CM grafts per cell delivered. Importantly, cardiac progenitor cells can

differentiate to not only hPSC-CMs but also other cardiac cell lineages such as endothelial cells and smooth muscle cells needed to generate viable cardiac tissue grafts. The first in human heart failure treatment clinical trial using hPSCs tested early stage hESC-derived progenitors delivered in a fibrin patch at the time of coronary artery bypass surgery and demonstrated safety for this preparation.[15] However, hPSCs undergo a dynamic range of cell state transitions in the process of differentiating to terminal cardiac lineages which are variably referred to as cardiac progenitors, and the specific characteristics of the given progenitor state chosen for cell therapy is critically important. The optimal cardiac progenitor cell population isolated from differentiating hPSCs and delivery strategy for cardiac repair remain to been determined.

Low cell retention is a vexing problem for all cardiac cell therapies. Our group previously described a cardiac extracellular matrix (cECM) engineered biomaterial using high-density culture-expanded cardiac fibroblasts isolated from human cadaveric hearts. cECM is an acellular, uniquely fibronectin abundant, non-chemically cross-linked, non-hydrogel scaffold with immunomodulatory and angiogenic properties that can be formulated into particulates, reconstituted into solution, and administered as an injectable[17, 18]. cECM was shown to educate monocytes to a distinct population of macrophages that exhibit anti-inflammatory and pro-angiogenic features,[18] and can promote myocardial retention of mesenchymal stem cells in rodent heart disease models when co-delivered epicardially via an open chest.[19, 20] In comparison, a more clinically appealing delivery approach is transendocardial injection (TEI). TEI uses a steerable, needle tipped catheter that is introduced into the left ventricle via a femoral artery to perform targeted intramuscular injections from the endocardial surface.

In this study, we tested whether human iPSC-derived committed cardiac progenitors (CCPs) alone or with cECM could be safely delivered to post-MI failing porcine heart and engraft to form cardiac tissue grafts that lead to improvements in functional outcomes. We found that the CCPs with or without cECM engrafted and differentiated to cardiomyocytes primarily and endothelial cells forming cardiac tissue grafts. Cardiac MRI did not show significant improvement in chamber size or ejection fraction, but pressure-volume analysis demonstrated an improvement in dobutamine stimulated functional reserve by CCPs. Cell delivery did not induce ventricular arrhythmias in the engrafted hearts.

METHODS

Committed Cardiac Progenitor Cells

Cryopreserved human iPSC-derived CCPs were obtained from Fujifilm Cellular Dynamics, Inc. (FCDI), Madison, WI. Briefly, the therapeutic grade iPSC line 31537.101 was reprogrammed from peripheral blood mononuclear cells (PBMCs) using proprietary FCDI technology and expanded to large master and working cell banks. Working cell banks were thawed into and expanded in multiple vitronectin-coated (ThermoFisher Scientific) CellSTACK® cell culture chambers (Corning), harvested with TrypLE (ThermoFisher Scientific), resuspended in Essential 8 Medium (ThermoFisher Scientific) containing H1152 (EMD Scientific) and CHIR99021 (Biovision) and seeded into 3L PBS3 MagDrive Bioreactors (PBS Biotech, Inc.) to initiate differentiation for large-scale cardiac progenitor cell manufacturing. Differentiation was achieved by modulating the Wnt/beta-catenin and TGFbeta/Actinin pathways using small molecules (CHIR99021, XAV939, SB43152) at specific timepoints during the process that included aggregate formation of

iPSCs, mesoderm induction, and specification towards a cardiac progenitor cell-fate. Approximately 4-6 x 10^9 CCPs were harvested from each bioreactor, dissociated with TrypLE, and cryopreserved with CryoStor CS10 (Biolife Solutions) at $300x10^6$ cells/5mL in AT-Closed Vials (Aseptic Technologies) using a controlled rate freezer and stored long-term in the vapor-phase of liquid nitrogen tanks.

In vitro differentiation potential of CCPs

CCPs were thawed directly into RPMI (ThermoFisher Scientific) + B27 supplement (1x) (ThermoFisher Scientific), washed, and resuspended in either RPMI+B27 for cardiomyocyte differentiation or Vasculife LS1020 (LifeLine Cell Technology) for endothelial differentiation. For cardiomyocyte differentiation, CCPs were plated into vitronectin-coated 6-well plates at $3x10^6$ cells/2mL/well or vitronectin-coated 96-well plates at $5x10^4$ cells/200uL/well. For endothelial differentiation, CCPs were either plated into diluted Matrigel coated T225 flasks at $3.4x10^6$ cells/45mL/flask or diluted Matrigel coated 12-well plates at $5x10^5$ cells/1mL/well. Respective cardiac or endothelial medium was refreshed 24hr post plating and every other day there-after until day 7 where the cells were washed with DPBS(-/-), and either fixed for immunocytochemistry or harvested with TrypLE to be re-plated or analyzed by flow cytometry.

Tube Formation assay

Day 7 CCP-derived endothelial cells were plated into undiluted Matrigel coated 24-well plates at various densities in 400 µl of Vasculife media/well. After 24 hr, cultures plated at 100k/well were imaged for tube formation using Nikon Eclipse Ts2 microscope with 4x objective.

Flow Cytometry

Cells were immunolabeled directly after thaw or after being harvested from *in vitro* differentiation assays. Cell surface protein expression was performed by labeling $2x10^5$ cells for KDR-PE (R&D Systems, FAB357P) + PDGFRα-APC (Cell Signaling, 5876S); CD56-APC (BD Biosciences, 555518) + CXCR4-PE (BioLegend, 306506); EpCAM-FITC (Miltenyi, 130-113-263); CD31-FITC (BD Pharmingen, 555445) + CD144-647 (BD Pharmingen, 561567); CD140b-PE (BD Pharmingen, 558821) + CD90-APC (BD Pharmingen, 559869) diluted in wash buffer (DPBS(-/-)+2% FBS) at 4°C for up to 60 minutes followed by washing and analysis with a BD Accuri flow cytometer. Intracellular protein expression was performed by staining $2x10^6$ cells with Live/Dead Green stain (Molecular Probes, L23101) for 15 minutes, washed, then fixed for 15 minutes with 4% formaldehyde. Fixed cells were washed twice with FACS permeabilization buffer (DPBS(-/-) + 0.1% saponin) and labeled with mouse anti-sarcomeric alpha-actinin (Abcam, ab9465) for at least 1 hour at 4°C. Cells are then washed twice with FACS permeabilization buffer, immunolabeled for 30 minutes with Alexa Fluor 647 donkey anti-mouse IgG (H+L) (ThermoFisher, A-31571), washed twice and analyzed with a BD Accuri flow cytometer.

Immunocytochemistry

Immunocytochemistry analysis for differentiation of CCPs to cardiomyocytes *in vitro* was performed using cells cultured in 96-well plates. Briefly, cells were washed with DPBS(-/-), fixed with 4% formaldehyde for 15 minutes and washed with ICC permeabilization buffer [DPBS (-/-) + 0.1% triton-X]. Cells were stained overnight at 4°C with mouse anti-sarcomeric alpha-actinin (Abcam) + rabbit anti-NKX2.5 (Cell Signaling) or mouse anti-

cardiac troponin T (ThermoFisher Scientific) + rabbit anti-cardiac troponin I (Abcam). The next day the cells were washed with ICC permeabilization buffer, stained with the appropriate Alexa Fluor donkey anti-mouse and anti-rabbit secondary antibodies for 30 minutes followed by nuclei staining with DAPI and imaged with an EVOS cell imaging system (ThermoFisher Scientific).

Immunocytochemistry analysis for differentiation of CCPs to endothelial cells was performed on cells cultured in 12 well plates. Briefly, the cells were washed with DPBS(-/-), fixed with 4% formaldehyde for 15 minutes and washed with ICC donkey perm-block buffer (DPBS(-/-) + (donkey serum)+ 0.2% saponin). Cells were then immunolabeled for 4hr at 4°C with sheep anti-CD31 (R&D Systems, AF806) + rabbit anti-cTNT (Abcam, ab45932). After primary incubation, cells were washed with ICC donkey perm/block buffer, labeled with the appropriate Alexa Fluor donkey anti-sheep 647 (Invitrogen, A21448) and anti-rabbit 488 (Invitrogen, A21206) secondary antibodies for 30 minutes followed by nuclei staining with NucBlue (Invitrogen, R37606) and imaged with Molecular Devices High content cell imaging system.

Gene Expression

Bulk RNA gene expression was performed in a two-step RT-PCR reaction followed by qPCR using the Fluidigm BioMark HD system. All steps were executed as described in Fluidigm's Real Time PCR Users Guide (68000088), appendix C. Briefly, 200 ng of total RNA prepared above was used as starting material for cDNA first strand synthesis using High Capacity RNA to cDNA kit (Applied Biosystems). The preamplification was done with TaqMan PreAmp Master Mix (Thermo Fisher Scientific) and 48 pooled primer pairs (50nM final concentration each primer) for 10 cycles (15 seconds at 95°C, 4 min at

60°C). Unincorporated primers were removed by Exonuclease digestion for 30 min at 37°C followed 15min inactivation at 80C (New England BioLabs). Samples were diluted 5-fold with DNA suspension buffer (Teknova). The qPCR was performed with Fluidigm's 48.48 dynamic array IFC on the Biomark HD using 2X SsoFast EvaGreen Supermix with Low Rox (Bio-Rad Laboratories), 20X DNA Binding Dye Sample Loading Reagent (Fluidigm), and primers at a final concentration of 500nM. The cycling parameters were as follows: hot start 95°C for 60 seconds, then 30 cycles of 96C for 5 sec, 60°C for 20 sec, followed by 60° – 95°C melting curve. cT values for gene expression values were generated and exported from Fluidigm Real-Time PCR analysis software. Relative gene expression values presented were normalized by RPL32 expression.

Cardiac fibroblast-derived Extracellular Matrix

Briefly, cECM (Tandem™, Cellular Logistics Inc, Madison, WI) was produced from primary human cardiac fibroblasts cultured under high-density conditions followed by a decellularization procedure as previously described.[17, 18] The injectable cECM formulation was manufactured by milling cECM scaffolds into a fine particulate of approximately 80-micron diameter using a pharmaceutical bead mill. cECM particles were added to the cell suspension and the cells are allowed to bind at room temperature for 1 hour prior to injection.

Closed Chest Porcine MI Model

All procedures were performed in accordance with a University of Wisconsin-Madison Institutional Animal Care and Use Committee approved protocol. Closed chest, 120 minute balloon-occlusion and reperfusion of the mid-left anterior descending artery was used to induce large anteroseptal MIs in male and female Yucatan swine (6-7.5 months

age, ~30kg, Premier Biosource, MI) using percutaneous methods previously described by our group[21, 22]. Amiodarone 25mg/kg po was administered daily starting 5 days pre-MI through 7 days post-MI. Heparin 70 U/kg IV was administered hourly during MI creation in all pigs. Lidocaine 50-100 mg/hr was administered as a constant rate infusion starting just prior to ischemia through to animal recovery. Amiodarone 50-100 mg IV, epinephrine 0.1-0.2 mg IV and external defibrillation at 200 J were administered as necessary to treat acute ventricular arrhythmias. Laboratory personnel and veterinary staff continuously monitored animals for their welfare before, during and after procedures. Pigs were survived 4 weeks post MI at which time they received the investigational treatment.

Experimental Design

There were two phases in the overall study. First, a roll-in, non-randomized cohort of pigs underwent direct epicardial needle injections of CCPs plus cECM into the infarct and peri-infarct region via an open chest thoracotomy to assess feasibility, establish best practices, and optimize immunohistochemistry to localize human cell grafts prior to launching the larger randomized-controlled trial. Following treatment, the roll-in cohort of pigs were survived for 2 weeks and then sacrificed. Arrhythmia surveillance and histopathology was performed; however, MRI and pressure-volume assessment were not performed since the primary objective was feasibility. Thereafter, an additional larger cohort of pigs were randomized by computer-generated block randomization into four treatment groups: 1) CCPs plus cECM, 2) CCPs alone, 3) cECM alone and 4) Control (Flexbumin), where the investigational products were administered by transendocardial catheter injections. Baseline MRI assessment was performed at 4 weeks post-MI followed by treatment. Four weeks after treatment, most pigs underwent cardiac MRI assessment followed by

invasive pressure volume hemodynamic evaluation and sacrifice. A small subgroup of pigs were survived to 8 weeks post treatment.

Epicardial Injections (Feasibility Cohort)

Due to the multi-faceted nature of this translational study, a small cohort of immunosuppressed post MI pigs underwent 10 epicardial injections of CCP+cECM into the infarct and peri-infarct border via an antero-lateral thoracotomy. Animals were recovered for 2 weeks, and then sacrificed. Detailed histopathology and continuous ECG recording was performed using an implantable ECG recorder (Reveal LinQ, Medtronic, Minneapolis, MN) that was surgically implanted in the skin adjacent to the left scapula. No MRI or pressure volume loop evaluation was performed in this small, single-arm feasibility cohort as its main purpose was simply to inform manufacturing feasibility, deliverability and to optimize tissue sectioning and immunohistochemistry staining methods.

Transendocardial Injections (Randomized Cohort)

An electroanatomical map of the left ventricle was performed with the NOGA XP Cardiac Navigation System (Biosense Webster) and NOGAstar mapping catheter to create an endocardial roadmap and distinguish viable from non-viable myocardium (**Supplemental Figure 2**).[23-25] An 8F electroanatomically tracked, deflectable TEI catheter with a 27G straight hollow needle design (Myostar, Biologic Delivery Systems, Irvine, CA) was used by an experienced operator who was blinded to the treatment assignment to perform the injections (**Supplemental Figure 2)**. Prior to initiating the injections, the needle injection depth was pre-calibrated to 3.5 mm when the catheter was placed in a curved in silico aortic arch with a 90-degree deflection. The injection strategy consisted of a total of 14

injections (200 microliter per injection) of study agent with approximately 50% of injections delivered into the peri-infarct borderzone and 50% directly into the infarct itself. Each injection was performed over 30 seconds with a 15-second dwell time.

Dose

Using aseptic technique, CCPs obtained from Fujifilm CDI, Madison, WI were rapidly thawed in a 37°C water bath (ThawSTAR, Biolife Solutions, Bothell, WA). 5% Flexbumin, which was used to suspend the cells and cECM, was used as a treatment control. Study agents were loaded into three, partially opaque 1 mL Luer lock syringes at room temperature. Intermittent gentle agitation was applied until injection. The total per pig CCP dose was 300 million CCPs and the total cECM dose was 50 mg.

Immunosuppression

To prevent immune rejection of the transplanted human cells, a 4 drug immunosuppression regimen was initiated prior to investigational treatment: i) cyclosporine 10 mg/kg po twice daily with adjustments to achieve trough levels above 250 microgram/L, ii) methylprednisolone 2.5 mg/kg po twice daily, iii) mycophenolate mofetil 250 mg oral twice daily and iv) abatacept 500 mg IV biweekly were administered. Sulfamethoxazole/trimethoprim 960 mg oral twice daily was administered to prevent infections. Blood samples were drawn every 2 weeks following investigational treatment for complete blood count, chemistry panel and cyclosporine levels.

Arrhythmia Surveillance

Continuous multi-lead telemetry monitoring was performed during MI model creation, investigational treatments, MRI and invasive P-V loop evaluation. An implantable ECG recorder (Reveal LinQ, Medtronic, Minneapolis, MN) was surgically implanted

subcutaneously adjacent to the left scapula at the time of the MI intervention using methods previously described by our group.[21] We previously confirmed that implanting these devices in this location was not associated with MR image distortion, and the magnetic field and radiofrequency did not interfere with ECG recordings.[21] The ECG recorder was programmed to detect: tachycardia>150 bpm for >24 beats, Asystole for >4.5 sec, Bradycardia <30 bpm for at least 4 beats and atrial fibrillation. Wireless device interrogation was performed on day 2, and then weekly post-MI. Rhythm strips from every recorded event were interpreted by an experienced clinical cardiologist (TJK) who was blinded to the treatment group assignment.

Magnetic Resonance Imaging (MRI)

Cardiac MRI was performed prior to treatment at baseline (4 weeks post-MI) and at 4 weeks post-treatment on a 3T Premier scanner (GE Healthcare, Waukesha, WI). Specifically, left ventricular chamber size and function was measured using short axis oblique slices with balanced steady-state free procession (bSSFP) imaging. (Scan parameters: TR/TE/Flip angle=3.3 ms/1.0 ms/50; field-of-view (FOV)/matrix=35×35 cm/200×224; slice thickness/spacing=10 mm/0 mm; cardiac phases/views per segment=20/16). Infarct size was measured using standard delayed enhancement (DE) inversion recovery based sequence performed 10 min following intravenous administration of 0.10 mmol/kg Gd-BOPTA (Multihance, Bracco Diagnostics, Princeton, NJ, scan parameters: TR/TE/TI/Flip angle=4.7 ms/1.0 ms/200–280 ms/25°; FOV/Matrix=35× 31.5 cm/224×192; slice thickness/spacing= 10 mm/0 mm; views per heartbeat=18). The trigger delay was adjusted to image mid-diastole based on the multiphase bSSFP series. All MRI imaging was performed at end expiration by temporarily suspending mechanical ventilation.

Anatomic and functional cardiac image analysis was performed by blinded personnel at the Radius Medical Imaging Analysis Core Laboratory using cvi42, Circle Cardiovascular Imaging, Calgary, CA. Cine bSSFP images were segmented to measure indexed LV end-diastolic volume, end-systolic volume, ejection fraction, stroke volume and radial, longitudinal and circumferential cardiac strain. Infarct size was quantified using late gadolinium enhancement imaging. Inclusion criteria for MRI evaluation was a 4 weeks post-MI ejection fraction of <45% or an infarct size of >9% of the LV size and freedom from sepsis or other severe infection.

Invasive Pressure Volume Assessment

Prior to sacrifice, invasive pressure-volume hemodynamic measurements were performed using a 5F high fidelity multi-ring electrode conductance catheter (Scisense Inc, London, ON) positioned retrograde into the left ventricle via transcarotid artery access. A 24 - 28 mm diameter balloon catheter was positioned via femoral vein into the inferior vena cava. Contralateral femoral venous access was obtained to advance a 7F Swan Ganz catheter under fluoroscopic guidance into the pulmonary artery. Calibrating stroke volume estimates were obtained by Swan Ganz thermal dilution method. Pressure–volume data was recorded at steady state and during transient inferior vena cava transcatheter balloon-occlusion, both at pre-dobutamine and with 20 mcg/kg IV dobutamine infusion using previously described methods.[21] Pre-load independent contractility reserve was defined as the difference in end-systolic pressure-volume relationship (ESPVR) between dobutamine stress and rest.

Myocardial contractility and work were indexed by the maximal rate of isovolumetric contraction (+dP/dt), stroke work (SW), and ventricular elastance, slope of the end-

systolic pressure–volume relationship (Ees). Pre-load was analyzed as end-diastolic volume and pressure and afterload evaluated as effective arterial elastance (the ratio of LV end-systolic pressure to stroke volume). Diastolic function was indexed by LV end-diastolic pressure and the time constant of ventricular relaxation (Weiss formula). Hemodynamic pressure–volume data was digitized at 200 Hz and stored for subsequent analysis on a personal computer by using commercial software (iWorx Dover, New Hampshire, USA).

Histopathology Assessment

Hearts were excised and hung on a modified Langendorf apparatus and perfused with 1 L heparinized saline followed by 1 L 10% neutral buffered saline. The hearts were then sectioned on the short access from apex to base in ~0.5 cm increments, then placed in 10 % neutral buffered formalin for 24 h before transfer to 70 % ethanol until histological processing. Histological analysis was carried out on one slide from each section. Fixed sections were co-immunolabeled for human species selective markers Ku80 and lineage specific markers including anti-TnI.

For each block, sections were prepared, and slides were analyzed independently by 3 experienced reviewers to identify and measure the area of human cardiomyocyte grafts using an EVOS (Life Technologies) microscope. When no grafts were identified on the slide, additional section cuts were made every 500 micrometers until human cardiomyocyte grafts were identified or until there was no tissue left in the block. The area of human cardiomyocyte grafts was measured manually by for the first section per block where grafts were identified.

Statistical Analysis

Statistical analysis was carried out using GraphPad Prism version 9. MRI data was analyzed with a 2-way ANOVA with a Sidak post-hoc analysis for multiple comparisons. Pressure volume loops were analyzed with a One-Way ANOVA with a Bonferroni post-hoc analysis. All data presented as mean +/- standard error. An alpha of 0.05 was considered significant.

RESULTS

Production of human iPSC-derived CCPs

For scalable production of human iPSC-derived CCPs, iPSCs were propagated as monolayer cultures in CELLSTACK culture chambers. Cells were singularized and inoculated into PBS3 Bioreactors to form cellular aggregates that were differentiated in suspension culture using an accelerated small molecule-based protocol employing biphasic modulation of Wnt signaling along with application of a rho-kinase inhibitor and TGF-β receptor inhibitor (**Figure 1A**). Flow cytometry analysis revealed a progressive loss of expression of the epithelial marker, EpCAM, present on iPSCs and upregulation of the mesodermal marker CD56 (NCAM) during the differentiation protocol (**Figure 1B**).[26] A $KDR^+/PDGFR\alpha^+$ population emerges and peaks at day 4 consistent with the generation of a cardiac progenitor population.[27, 28] KDR expression subsequently decreases on day 5 and 6 suggesting advancing maturation of these cardiac progenitors. Analysis of gene expression over the 6-day protocol revealed loss of expression pluripotency genes (*NANOG, SOX2, POU5F1)* and an increase in expression of cardiac progenitor genes (*HAND2, GATA4, NKX2-5, PDGFA, TBX5*) (**Figure 1C**). At day 6, the aggregates are dissociated, cryopreserved and described as CCPs.

In vitro potency of CCPs

To test the potency of the cryopreserved CCPs, cells were thawed and plated on vitronectin substrate in RPMI+B27 medium and characterized after 7 days of culture. The starting cell population expressed CD56 and PDGFRα but not KDR nor sarcomeric α-actinin, consistent with a CCP cell population (**Figure 2A**). After 7 days in culture in RPMI+B27, the cells differentiated into contracting sheets of iPSC-derived cardiomyocytes (iPSC-CMs) (Video supplement 1). Flow cytometry demonstrated that 96.3±0.9% of the differentiated cells were iPSC-CMs based on sarcomeric α-actinin (SAA) expression (**Figure 2B**). Immunolabeling of the differentiated cells confirmed that nearly all cells were iPSC-CMs which expressed Nxk2.5, SAA, cardiac troponin I (cTnI), and cardiac troponin T (cTnT) (**Figure 2C**). These results show that thawed CCPs plated in basal RPMI+B27 medium without additional growth factors or small molecules rapidly differentiate predominantly to iPSC-CMs.

To determine the potency of CCPs to differentiate into iPSC-derived endothelial cells (iPSC-ECs), thawed CCPs plated as above in RPMI+B27 for 7 days were characterized by flow cytometry for expression of the EC markers CD31 and CD144 (VE-cadherin). No CD31 or CD144 positive cells were observed. However, if the thawed CCPs were plated in an endothelial medium, Vasculife LS1020, after 12 days, a large CD31 and CD144 double positive population of iPSC-ECs was present (**Figure 2C**). Immunolabeling of the day 12 cultures also demonstrated expression of CD31 in a monolayer of human iPSC-ECs. To test the functional properties of the iPSC-ECs, a matrigel tube formation assay was carried out on replated day 12 cells. One day after replating, the iPSC-ECs organized into an interconnected network of tubes in Matrigel. Thus, in medium optimized for EC culture, CCPs readily differentiate to iPSC-ECs.

<u>CCPs engraft in swine infarcted myocardium and differentiate to cardiac lineages</u>

A total of 70 pigs underwent LAD balloon occlusion reperfusion, of which 50 survived the post-MI period to treatment (71%) (**Supplemental Figure 1**). Of the remaining 50 pigs, 6 pigs were evaluated in the roll-in feasibility cohort which underwent open-chest epicardial injections of CCPs+cECM after 4 weeks post-MI. Pigs were sacrificed 2 weeks later, and hearts were sectioned for histopathology. The other 44 pigs were randomly assigned to one of four treatment groups: CCP+cECM, CCP alone, cECM alone or Control (5% Flexbumin). Entry of pigs into the cECM alone cohort was stopped after only 3 pigs were treated due to lack of a clear trend toward improved ejection fraction and limitations on animal numbers. Thus, the functional studies focused on comparing 3 groups: CCPs, CCPs+cECM, and control.

In the feasibility roll-in cohort, pigs were followed for 2 weeks post cell delivery, and the presence of engrafted human cells was assessed by immunolabeling for human nuclear antigen, Ku80, or human mitochondria. All 6 pigs demonstrated Ku80 positive human cell grafts that were composed largely of cTnI co-labeled cells; however, cTnI labeling intensity was less than observed in the native pig myocardium (**Figure 3A**). Trichrome staining of an adjacent section revealed the corresponding human cell grafts adjacent to the native myocardium (**Figure 3B**). Human cell grafts were identified within the scar, in adjacent native myocardium and also on the epicardial surface (**Figure 3C-E**). The grafts were composed predominantly of human cardiomyocytes based on the cTnI immunolabeling, but the sarcomeric pattern and density of labeling was consistent with immature cardiomyocytes. In addition, using co-labeling with an antibody detecting human mitochondria and an antibody for CD31, we detected human endothelial cells in the grafts (**Figure 3F-I**). These results demonstrate that the CCPs can survive following

injection into the post-MI porcine heart and differentiate into cardiomyocytes and endothelial cells to form cardiac tissue grafts.

In the randomized phase, pigs were sacrificed at 4 weeks post-treatment, although a small subset of pigs were survived to 8 weeks after transendocardial delivery. In pigs receiving CCPs with or without cECM, hearts were systematically blocked, and sections were immunolabeled for human Ku80 and cTnI. Human grafts were identified in 12/13 (92.3%) and 11/12 (91.6%) of pigs in the CCPs and CCPs+cECM cohorts, respectively. The transendocardial delivery strategy targeted 50% of the injections to the infarct zone and 50% to the borderzone, and we observed approximately 50% of the grafts in the borderzone (**Figure 4A**). However, the remaining grafts were detected not only in the infarct zone, but also on the epicardial surface of the heart. Epicardial grafts were significantly more common in the CCP+cECM group. The graft areas observed on the histological blocked sections were comparable between the CCP and CCP+cECM groups (0.68 +/- 0.27mm^2 and 0.42 +/- 0.18 mm^{2,} respectively, p=0.45) Macroscopic graft size was not measured given the blocking strategy used to enable detailed histological characterization of the large porcine hearts. There was no difference in the observed cellular composition of the grafts present in the CCP compared to the CCP+cECM treated animals with grafts composed almost exclusively of cTnI$^+$ cardiomyocytes with occasional human endothelial cells detected. Grafts were present in both CCP and CCP+cECM animals up to the latest time point sampled, 8 weeks after delivery.

<u>CCP-derived grafts show progressive maturation of ventricular cardiomyocytes</u>

To assess the chamber-specificity of the differentiated cardiomyocytes in the grafts and to examine for evidence of maturation, we immunolabeled sections with an antibody

recognizing the ventricular-specific myosin light chain, MLC2v at 2-, 4- and 8-weeks post-transplant. Almost all of the human cells identified using an anti-human mitochondrial antibody expressed MLC2V at all time points tested (**Figure 4B-G)**. There was evidence of progressive sarcomere organization and maturation based on the pattern of MLC2v labeling from 2 weeks to 8 weeks, although the cells remained smaller and with less sarcomere organization than adjacent adult porcine myocardium. Together these results demonstrate that transendocardial delivery of CCPs in the post-MI swine heart leads to formation of cardiac grafts predominantly composed of human ventricular cardiomyocytes with occasional human endothelial cells. The grafts persist for the 8 weeks of observation in this immunosuppressed swine model and show evidence of progressive cardiomyocyte maturation.

Cardiac MRI Assessment

Twenty-two pigs were evaluable for MRI in the three experimental groups, whereas 19 pigs were excluded from the MRI analysis due to: LVEF >45% (n=1), infarct size <8% of LV (n=1), hemodynamically significant opportunistic sepsis/infection (n=13), and technical issues with the MRI acquisition (n=4) (see **supplemental Figure 1**). Prior to CCP delivery, there was no significant difference in baseline post-MI left ventricular ejection fraction: CCPs alone (n=5) 43.8 +/- 4.3%, and CCPs+cECM (n=9) 39.9 +/- 4.1%, and Control (n=8) 44.8 +/- 4.2%. Four weeks following transendocardial delivery, no statistically significant change in ejection fraction was observed for any of the three groups, but CCPs trended to improvement (p=0.08), while CCPs+cECM (p=0.3) and control injections (p=0.99) showed no clear improvement (**Figure 5A,B)**. Similarly, there was no statistically significant difference between groups in left ventricular end-diastolic volume and left ventricular end-systolic volume following intramyocardial injection (**Figure**

5C,D). Late gadolinium enhancement-determined infarct volume was not significantly changed in any of the three groups (**Figure 5E,F)**.

CCPs and CCP+cECM Improve Contractility Reserve

Invasive hemodynamic pressure-volume (PV) studies were performed at the endpoint of the study for each animal. Only pigs meeting the MRI inclusion criteria above (EF<45% or infarct >9% of LV, free of infection) were considered potentially evaluable by PV loop analysis. Technical problems during PV-loop acquisition or poor-quality loops caused the exclusion of 9 additional animals. Comparison of resting ejection fractions from the hemodynamic studies demonstrated a significantly higher ejection fraction in the CCP (46.1 ±1.5%) group compared to Control (34.6 ±3.0%) (p=0.007), and the CCP+cECM (41.7 ±1.7%) group showed a trend to improvement (**Figure 6D)**. End systolic volume was significantly reduced in CCP (46.4 +/-3.5 ml) and CCP+ECM (48.9 +/-2.7 ml) groups compared to Control (75.9 +/-4.9 mL) (p=0.0001 ANOVA; p=0.001 and p<0.0001 respectively). End diastolic volume was also significantly reduced in CCP (86.3 +/- 6.3 ml) and CCP+ECM (84.0 +/-4.4 ml) groups compared to the Control group (116.5 +/-5.7 ml) (p=0.025 ANOVA; p=0.004 and p=0.0005 respectively). There was no significant difference in end systolic elastance between CCP, CCP+ECM and Control groups at baseline (p=0.16 ANOVA). However, following dobutamine challenge to assess contractile reserve, a significant increase in elastance in both CCP alone (7.6 +/-1.1) and CCPs+cECM (5.4 +/-0.9) and control (compared to baseline (p=0.004 and p=0.002 respectively) was observed but not in the Control group (4.0 +/-0.7) (p=0.28). The CCP and CCP+cECM showed significantly greater elastance in the presence of dobutamine relative to Control (p<0.05)

Safety evaluation shows no CCP-induced ventricular tachycardia

Safety assessment for the study included evaluation of procedure related complications, gross or histological tumor formation, and arrhythmias. In all treated pigs, there were no procedure related adverse events such as sustained ventricular tachycardia (>30 seconds), cardiac perforation, MI, stroke, or limb ischemia. Continuous electrocardiographic monitoring for significant tachycardia (>150 bpm) using an implanted cardiac monitor (LINQ) was performed from the time of the initial MI until pigs were sacrificed, in both the initial feasibility cohort and the randomized cohort. There was only one episode of sustained ventricular tachycardia (>30 seconds) that self-terminated in one randomized cohort pig treated with CCP+cECM on post-injection day 2 (**Supplemental Figure 3**). Otherwise, there were no episodes of sustained ventricular tachycardia (>30 seconds) or ventricular fibrillation detected in any of the other pigs during the treatment injection procedures and for up to 8 weeks of follow-up. Finally, necropsy did not reveal evidence of gross tumors in any animal and there was no cardiac histological evidence of tumor formation observed.

DISCUSSION

In this preclinical study, we tested the ability of minimally invasive TEI delivery of a novel human iPSC cell product, CCPs, alongside a retention biomaterial to remuscularize the porcine post-MI myocardium. The major findings are: i) transplanted CCPs differentiate to form grafts composed primarily of cTnI and MLC2v positive ventricular cardiomyocyte and occasional human CD31 positive endothelial cells, ii) neither transplant of CCPs or CCPs+cECM significantly improved cardiac MRI measured ejection fraction or cardiac volumes, but the CCP and CCP+cECM groups demonstrated significantly greater

contractility reserve relative to control by invasive hemodynamic assessment, iii) CCP +/- cECM administration was feasible without adverse safety outcomes including no tumor formation and no ventricular arrhythmias, and iv) human iPSC-CMs in grafts displayed progressive maturation but remained structurally immature at 8 weeks post injection. Together, these results demonstrate that CCPs hold promise as a therapy for the post-MI heart.

The concept of using cardiac progenitor cells for post-MI heart failure treatment has been investigated in a variety of contexts. The adult heart does not contain a pool of stem or progenitor cells with potency to generate new heart muscle,[29, 30] but hPSCs provide an accessible and clinically relevant source of cardiac progenitor cells. However, hPSC-derived cardiac progenitor cell populations are heterogenous and dynamic during differentiation akin to cardiac development in which different progenitor populations gradually give rise to distinct heart regions and structures. An early study using *in vitro* engineered heart tissue comparing mouse ESC-CMs and ESC-derived Flk1$^+$/PDGFRα$^+$ cardiac progenitor cells demonstrated that the cardiac progenitor cells differentiated to CMs and improved the electrical coupling in the engineered heart tissue more effectively than the ESC-CMs.[31] Using similar cell preparations from hESCs, a study comparing hESC-CMs to KDR$^+$/PDGFRα$^+$ cardiovascular progenitor post-MI in a nude rat model showed comparable grafts and functional effects from the two populations.[32] A developmentally earlier mesodermal SSEA1$^+$ cell population derived from rhesus ESCs was shown to engraft and differentiate to cardiomyocytes, populating 20% of the scar region in the post-MI rhesus heart.[33] However, a more recent study of the xenogeneic transplantation of hESC-derived SSEA1$^+$ post-MI nonhuman primate hearts found no human cells remaining at 140 days, although an improvement in cardiac function was

observed and attributed to decreased apoptosis of endogenous cardiomyocytes.[34] Studies using an intermediate stage cardiac progenitor population first identified by high levels of Isl1 expression showed in rhesus heart slice models that the cardiac progenitors are highly migratory and can track to areas of cryoinjury.[35] In post-MI porcine model, the same cardiac progenitors engrafted and formed cardiomyocyte rich grafts, but there was no statistically significant improvement in MRI measures of LV function after 12 weeks.[35] Yap et al.,[16] provided evidence that late-stage or committed cardiac progenitors can be effectively delivered at the time of surgically induced MI, engraft and differentiate to relevant cardiac lineages forming cardiomyocytes rich grafts lasting at least 2 months with evidence for improvement in EF from cardiac MRI.[16] However, the study by Yap et al., found evidence for ventricular arrhythmias following cell delivery in approximately half of the treated animals.[16] In the present study, we used late stage CCPs, but unlike prior studies they were differentiated from hiPSCs rather than hESCs. Secondly, the present study used clinically relevant TEI delivery in contrast to prior studies using surgical, epicardial injection. Comparable to earlier studies, we observed engraftment and differentiation to form cardiac muscle grafts, but there was not an improvement in cardiac function on cardiac MRI evaluation despite an improvement in dobutamine recruitable functional reserve. In summary, studies using hPSC-derived cardiac progenitor cells in animal models post-MI demonstrate the ability of the cells to engraft and differentiate with variable evidence for improvement in cardiac function and risk of ventricular arrhythmias.

Significant safety concerns due to ventricular arrhythmias following delivery of hPSC-CMs by epicardial injection in large animal post-MI heart failure models have arisen, although the arrhythmias are generally transient, starting 1 week after transplant and lasting approximately one month.[10, 12, 14] Current evidence suggests that these ventricular

arrhythmias are the result of automaticity arising from the graft CMs rather than reentry mechanisms. The sustained ventricular tachycardia has been tolerated in nonhuman primate models following cell therapy, but in porcine models, there has been significant mortality observed in treated animals.[10, 36] Pharmacological treatment with ivabradine and amiodarone reduced the engraftment arrhythmia burden but did not eliminate it.[36] Given that abnormal automaticity is the presumed basis for these ventricular arrhythmias, gene editing was used to alter expression of 4 different ion channels and transporters to eliminate automaticity. This approach greatly reduced engraftment arrhythmias, although there was still an early period of sustained ventricular tachycardia. The arrhythmic risk for cardiac progenitor cells is less clear as some of the large animal studies did not directly monitor for arrhythmias. However, Yap et al. observed that approximately half of the treated pigs with CCPs developed sustained ventricular tachycardia starting 9 days or later and lasting at least a month and in one animal up to week 12, which appears slightly delayed relative to the hPSC-CM studies. This potentially reflects the additional time needed for differentiation of CCPs. In contrast, the present study failed to observe sustained ventricular tachycardia in any CCP treated animal. The underlying reasons for the difference in arrhythmic risk observed in these two CCP studies will require further investigation, and potential considerations include differences in the cell population, TEI vs. epicardial delivery, or time after MI for therapy. Ultimately identifying the key factors that eliminate or minimize the arrhythmia risk is necessary for this therapy to advance to the clinic.

Combining cell products with matrix preparations or synthetic hydrogels has been demonstrated in previous studies to improve cell retention and survival in post-MI hearts. For example, the pro-survival cocktail used in several studies includes the complex matrix

preparation, Matrigel™.[5] Gelatin hydrogels have been used successfully in the transplantation of iPSC-CM cardiomyocytes spheroids in post-MI animal models.[37] In this study, we tested the addition of an injectable formulation of cECM to the CCP product, but this did not result in improved functional benefits; however, we did find an increase in the number of epicardial grafts on the surface of the heart in the cECM+CCP group relative to CCP alone. This may be related to cECM helping retain any cells that get into pericardial space. How this potential differential localization of grafts impacts long-term outcomes will require additional study. In addition, cECM has been proposed to have favorable immunomodulatory effects via alternatively activated macrophage education,[18] which could theoretically make local, ischemic tissue more hospitable for co-transplanted cells. However, these favorable influences may be blunted in this immunosuppressed animal model. Overall, the tested delivery of cECM did not improve functional outcomes in this study, but additional studies are needed to determine the optimally formulated and dosed delivery vehicle to promote cell survival and engraftment.

TEI delivery has emerged as an appealing, minimally invasive approach for direct intramyocardial transplantation of cells, biomaterials and other biologic agents in a targeted fashion. In a recent pooled analysis, this delivery approach was observed to be overall safe in >1800 patients injected in clinical trials worldwide[38]. In this study, the NOGA/Myostar (Biosense Webster/J&J) mapping and TEI catheter platform was used to perform targeted injections; however, this platform was recently discontinued from production by the manufacturer. Alternative cardiac mapping approaches to facilitate accurate targeting with TEI, such as co-registered multimodality imaging, have been described but remain investigational.[22] Similarly, alternative investigational TEI catheters, such as the helical needle-tipped “Helix” catheter (BioCardia, Sunnyvale, CA), are being

actively used in active adult cell therapy trials[39, 40]. These novel cardiac visualization methods and catheter designs may pave the way to help inject a new generation of therapeutic cells designed to remuscularize the damaged heart.

Overall, the optimal hPSC cell product and delivery strategy to remuscularize the heart remains to be determined. Even a combination of cell products may be preferable such as hiPSC-derived endothelial cells and hiPSC-CMs to promote cell survival and revascularization.[41] Ground breaking phase 1 clinical trials are testing hPSC-CMs to treat heart failure employing epicardial injections,[42] transcatheter injections (NCT04982081) and epicardial patches (NCT04945018, NCT04396899) are underway world-wide as well as a completed trial demonstrating the safety of hESC-SSEA1^{+} progenitor cells transplanted at the time of coronary artery bypass grafting surgery.[15] Despite these developments, important unanswered questions remain including concerns about immunogenicity, repeat dosing possibilities, electromechanical integration, arrhythmogenicity, and whether minimally invasive transcatheter administration will be feasible for wider adoption of this therapy.

Nevertheless, early phase clinical trials are underway testing the safety of delivering hPSC-CMs in patients with heart failure with reduced ejection fraction either by direct intramuscular injection or transplantation of cellularized sheets to the epicardium [clinicaltrials.gov NCT03763136; NCT04945018; NCT03763136; NCT04696328; NCT04945018].

Limitations

The current study did not provide long-term follow-up of the animals, in part due to the challenge of opportunistic infections in the setting aggressive immunosuppression.

Infections also caused a reduction in the planned sample size. Electrical integration of the cells was not directly examined in this study, but it will be an important subject of future research to define the mechanisms leading to lack of arrhythmias in our study relative to hPSC-CMs studies.

Acknowledgements:

Sincere thank you to Allison Rodgers, Everett Temme, Sarah El Meanawy and Vivian Hacker for animal handling and procedures, and Emily Ferris for MRI acquisition and analyses.

Sources of Funding

Funding support provided by:

1. National Institutes of Health 5U01HL148690-02
2. National Institutes of Health T32 HL007936
3. Fujifilm Cellular Dynamics, Inc, Madison, WI
4. Cellular Logistics, Inc., Madison, WI
5. University of Wisconsin-Madison

Disclosures

ANR: Research or educational grants from Fujifilm Cellular Dynamics, Siemens Healthcare, BioCardia. Consultant for Blue Rock Therapeutics and Novo Nordisk. Co-founder with equity interest in Cellular Logistics, Inc.

EGS: Co-founder with equity interest in Cellular Logistics, Inc.

CK, MB, KS, and EH are employees of Fujifilm Cellular Dynamics, Inc.

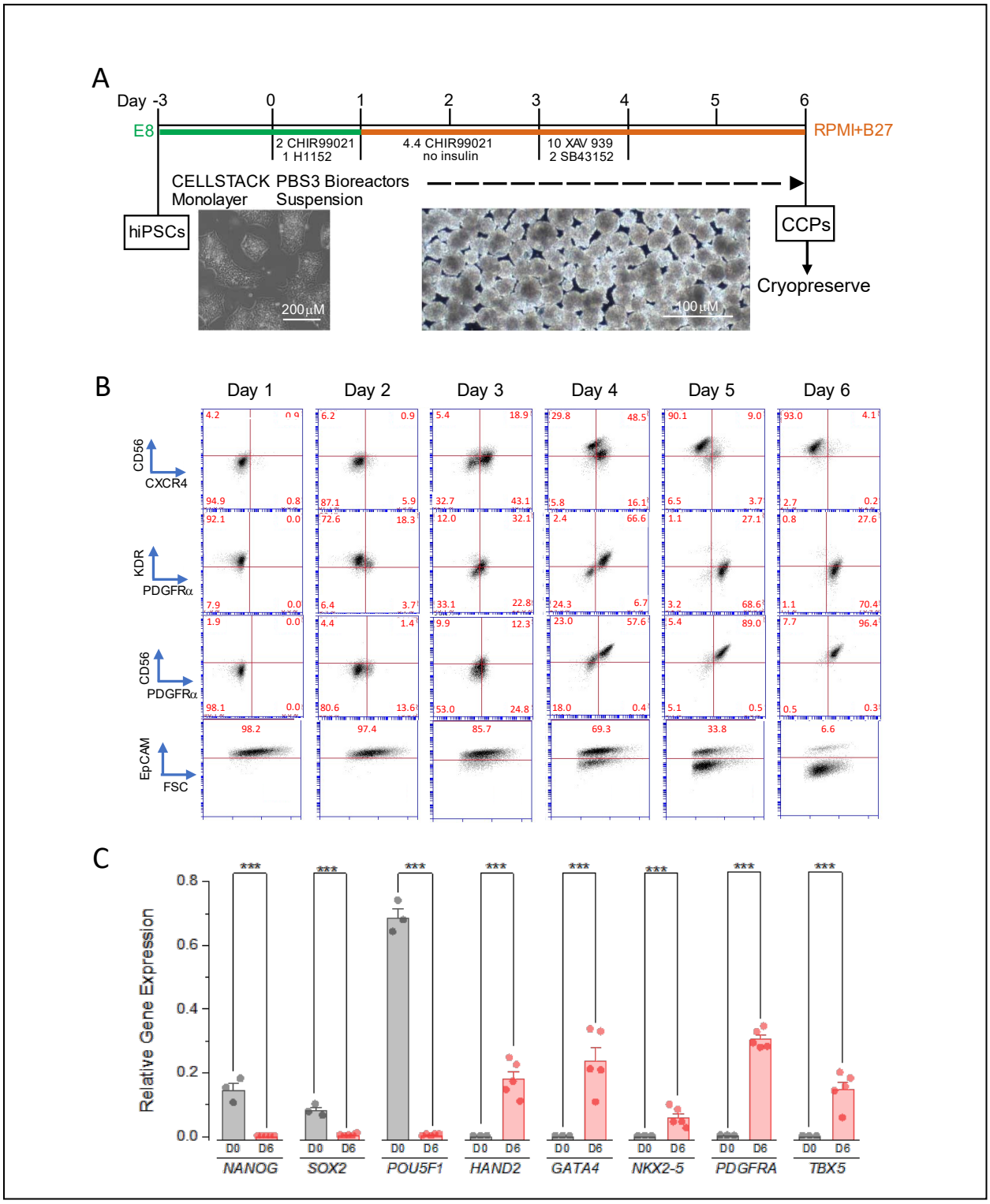

Figure 1. Differentiation of human iPSCs to CCPs. A) Differentiation schematic to manufacture CCPs with images showing starting aggregates of human iPSCs and final aggregates of CCPs. **B)** Time course of differentation characterizing cell surface protein expression of CD56, KDR, PDGFRα, and EpCAM using flow cytometry. **C)** Gene expression of pluripotent and cardiac-specific genes at day 0 (iPSCs) and day 6 (CCPs) relative to the ribosomal protein *RPL32*. ***p<0.005 by t-test comparison.

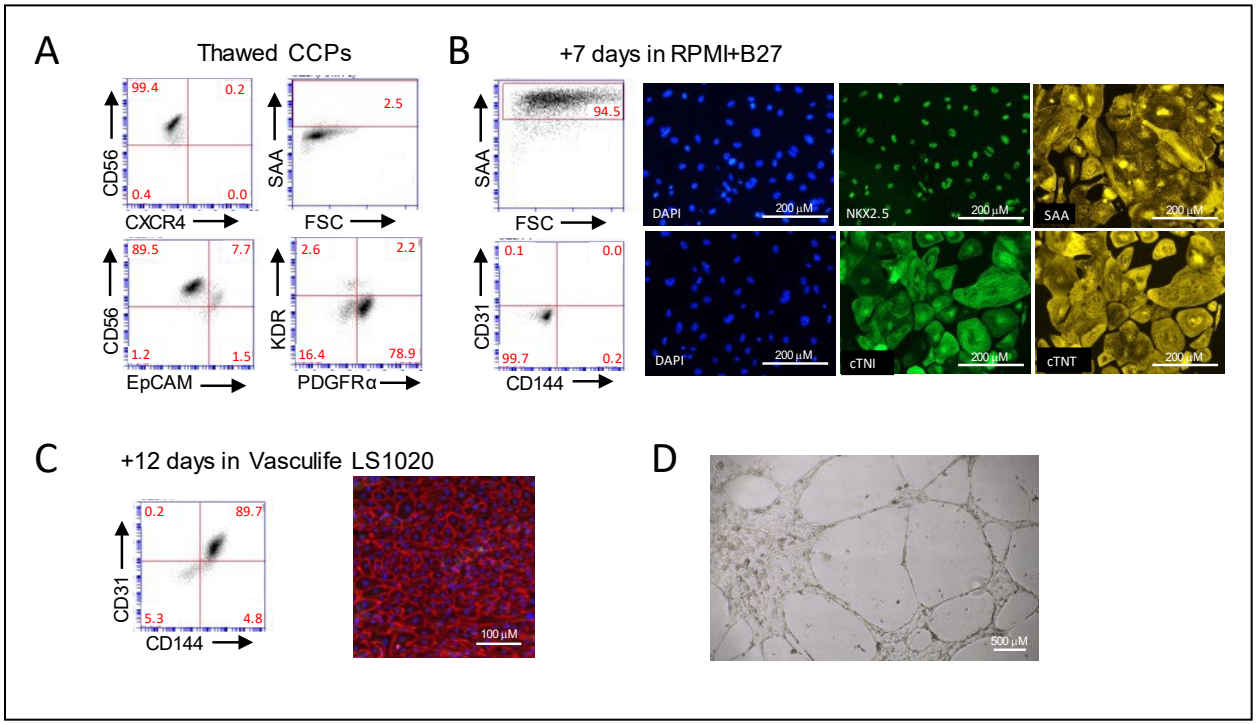

Figure 2. **In vitro differentiation of CCPs to iPSC-CMs and iPSC-ECs**. **A)** Flow cytometry for cell surface markers (CD56, CXCR4, KDR, PDGRFα) and the cardiomyocyte-specific sarcomeric α-actinin (SAA) protein expression directly after thawing the CCPs. **B)** Seven days after plating CCPs on vitronectin in RPMI+B27 analysis by flow cytometry (left panel) for cardiomyocyte (SAA) and immunofluorescence labeling (right panels) for cardiomyoctye markers Nkx2.5 SAA, cardiac troponin I (cTnI) and cardiac troponin T (cTnT). **C)** Twelve days after plating CCPs in Vasculife LS1020 media analysis by flow cytometry for endothelial markers CD31 and CD144 and immunolabeling (right panel) for CD31. **D)** Dissociated day 12 cells in Vasculife LS1020 plated for one day in undliluted Matrigel form tubes.

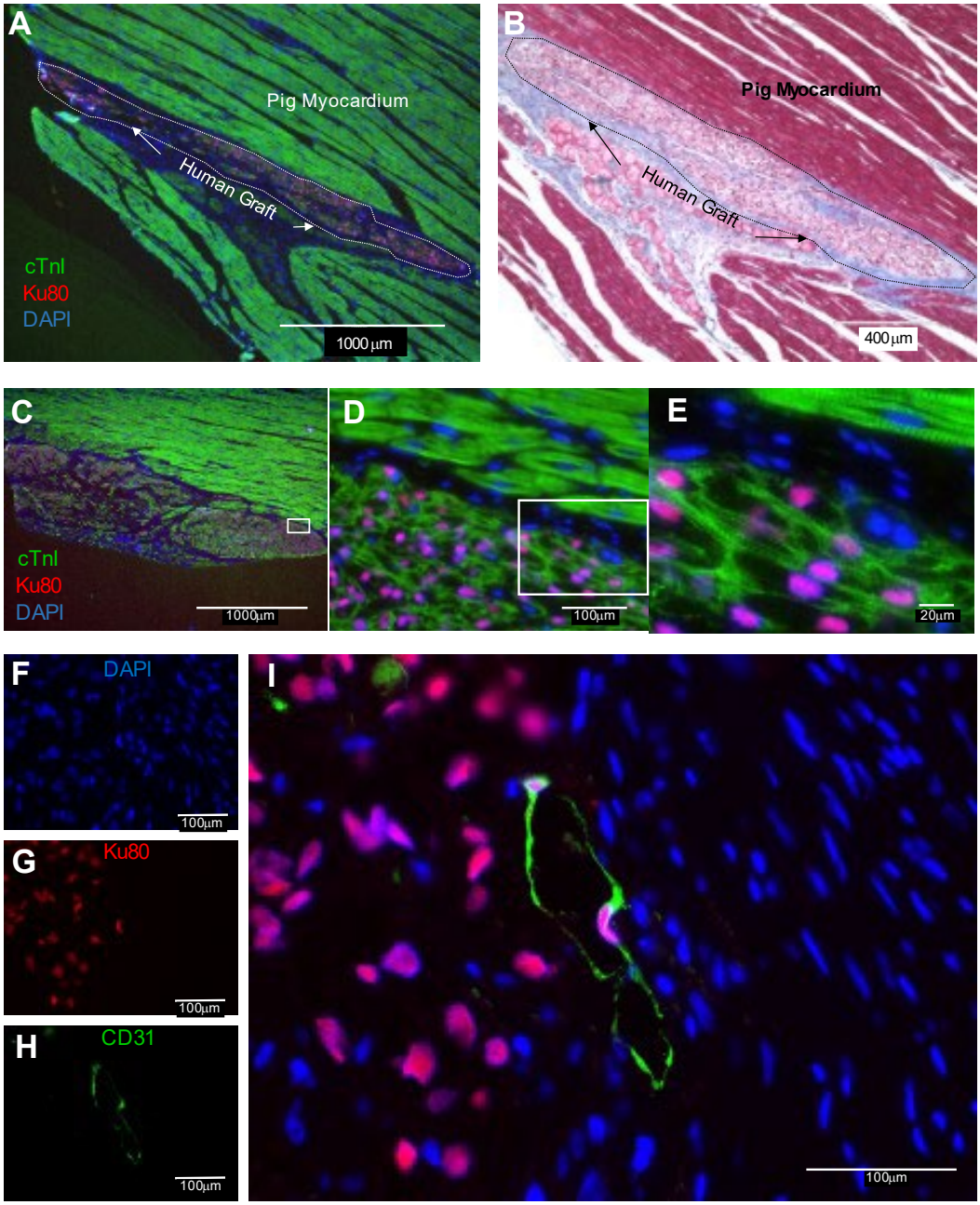

Figure 3. iPSC-CCPs engraft and differentiate to cardiomyocytes and endothelial cells 2 weeks after delivery in post-MI swine heart. A) Epifluorescence image of porcine heart section with human graft identified by Ku80 immunolabeling and cardiomyoctyes by cTnI immunolabeling. **B)** Light microscopic image of adjacent histological section stained with Mason's Trichrome. **C-E)** Immunofluorescence images of human graft in porcine myocardium immunolabeled as indicated identifies human cardiomyocytes. **F-I)** Immunofluorescence image of another human graft in porcine myocardium labeled with anti-Ku80 and anti-CD31 to identify human endothelial cells in the graft.

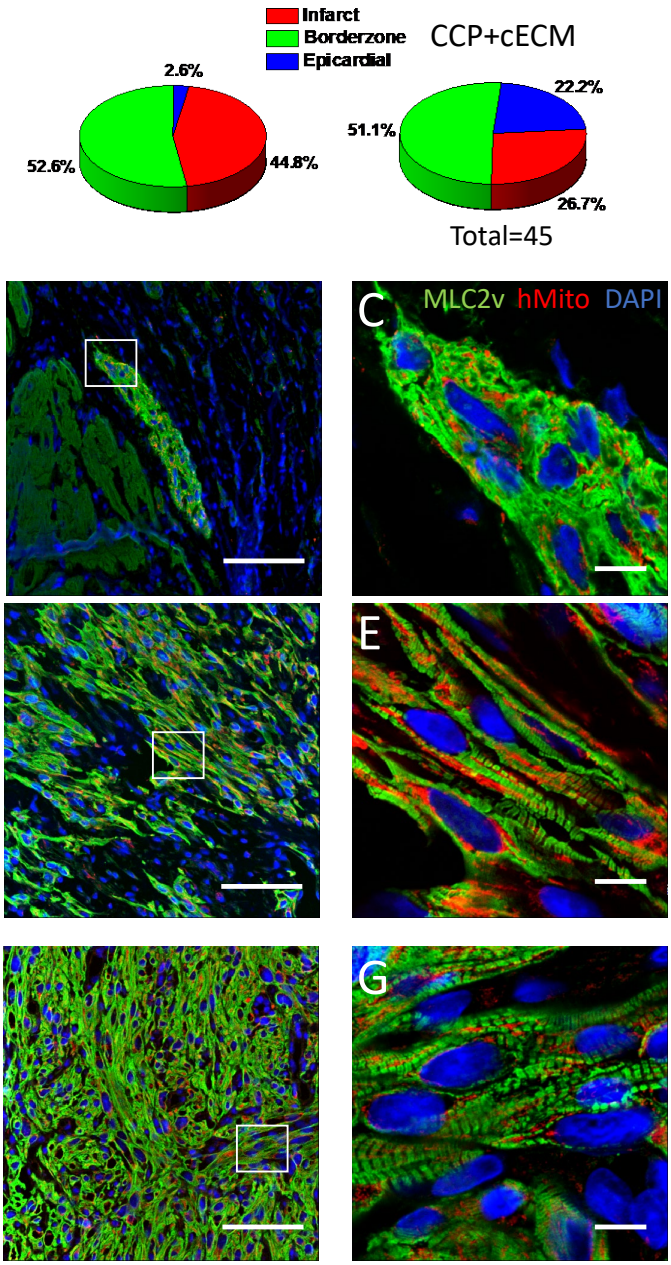

Figure 4. CCP graft localization and maturation of MLC2v expressing ventricular-like cardiomyocytes over 8 weeks. A) Distribution of histologically detected human grafts based on Ku80 labeling following transendocardial delivery of CCPs to 12 animals or CCP+ECM in 13 animals. The distribution is significantly different (p=0.019 by Chi-square test) with CCP+cECM animals showing more epicardial grafts and fewer in the infarct region. **B-G)** Confocal immunofluorescence imaging showing CCP-derived grafts at time points indicated post-delivery labeling labeled with ventricular-specific MLC2v, human mitochondrial antibody and DAPI. Left row scale bar 200 μm, and right row expanded inset from indicated region in white box with scale bar 10 μm.

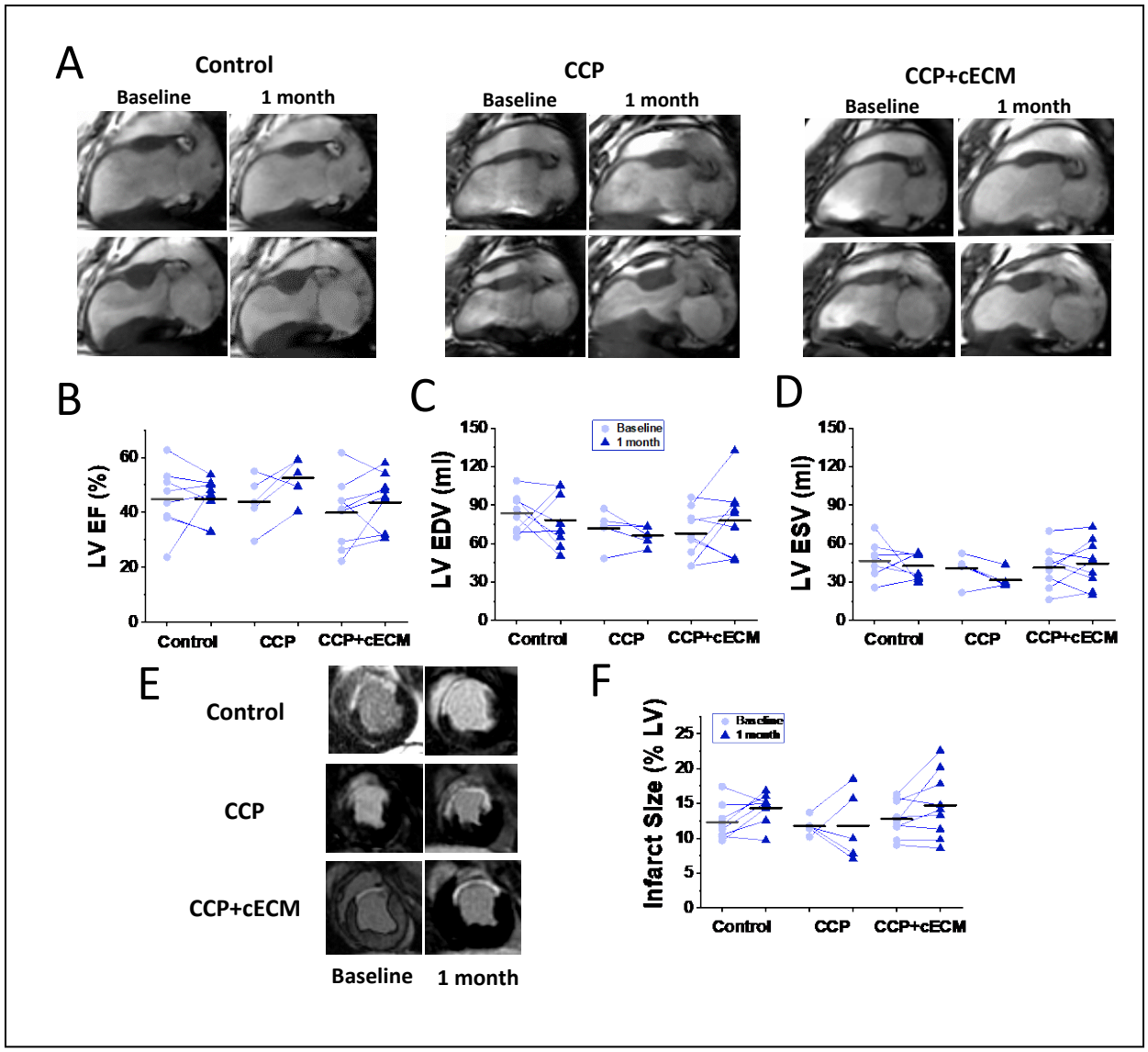

Figure 5. Cardiac MRI analysis. A) Representative diastolic (upper) and systolic (lower) cardiac cine MR images from Control, CCP only and CCP+cECM treated animals. **B-D)** Comparisons of baseline and 4 weeks after treatment of LVEF, LVEDV and LVESV showed no statistically significant differences between groups. **E)** Representative cardiac MRI viability images. **F)** Comparisons of baseline and 4 weeks MRI infarct size showed no significant differences.

CCP = committed cardiac progenitor cells, cECM = cardiac extracellular matrix, LVEF = left ventricular ejection fraction, LVEDV = left ventricular end diastolic volume, LVESV = left ventricular end systolic volume.

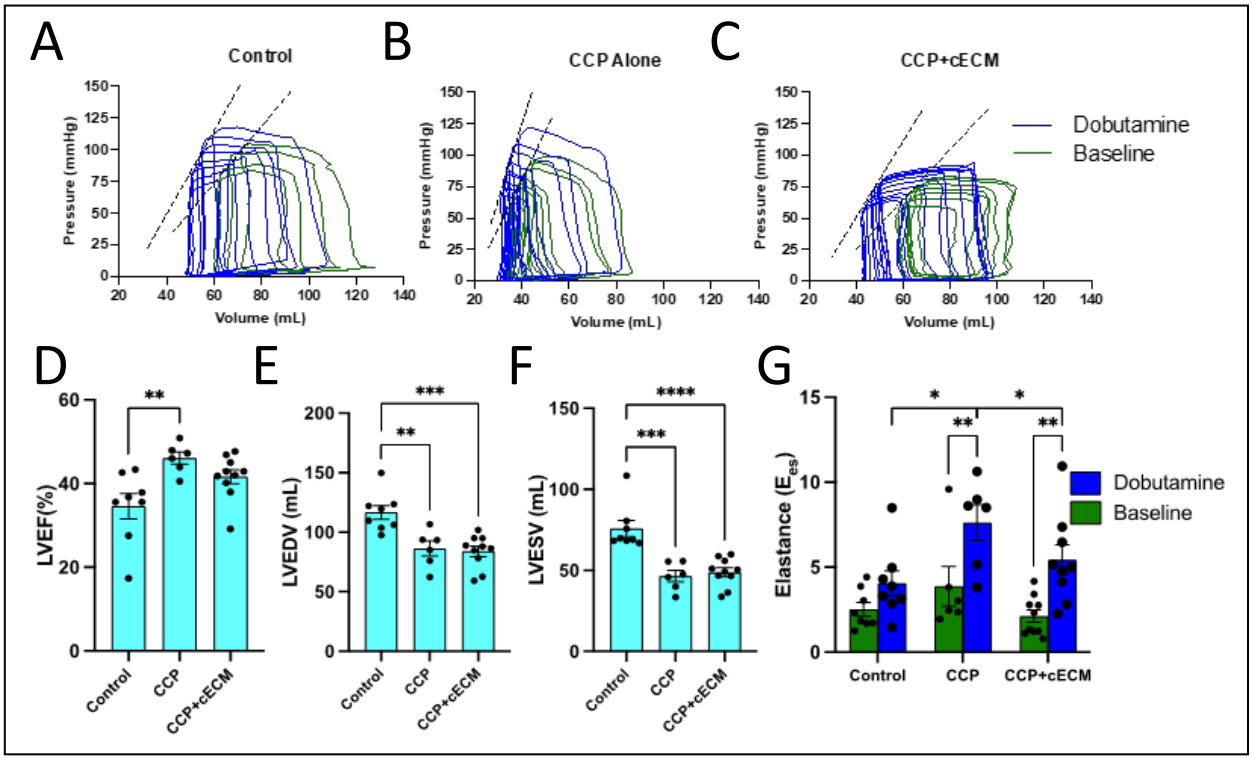

Figure 6. Invasive hemodynamic analysis demonstrates CCP and CCP+cECM show reduced left ventricular volumes and improved contractile reserve. A-C) Representative pressure-volume loop recordings of baseline-dobutamine stress from Control, CCP and CCP-cECM treated pigs at 4 weeks following treatment. **D)** LVEF was significantly greater in the CCP group compared to Control. **E)** LVEDV was significantly reduced in CCP and CCP+ECM relative to Control. **F)** LVESV was significantly reduced in CCP and CCPP+ECM groups relative to Control. **G)** End systolic elastance determined from pressure-volume recordings at baseline and after dobutamine show increased contractile reserve in the CCP and CCP+cECM groups.

CCP = committed cardiac progenitor cells, cECM = cardiac extracellular matrix, LVEF = left ventricular ejection fraction, LVEDV = left ventricular end diastolic volume, LVESV = left ventricular end systolic volume *p≤0.05, **p≤0.01, ***p≤0.0001

Supplemental Figures

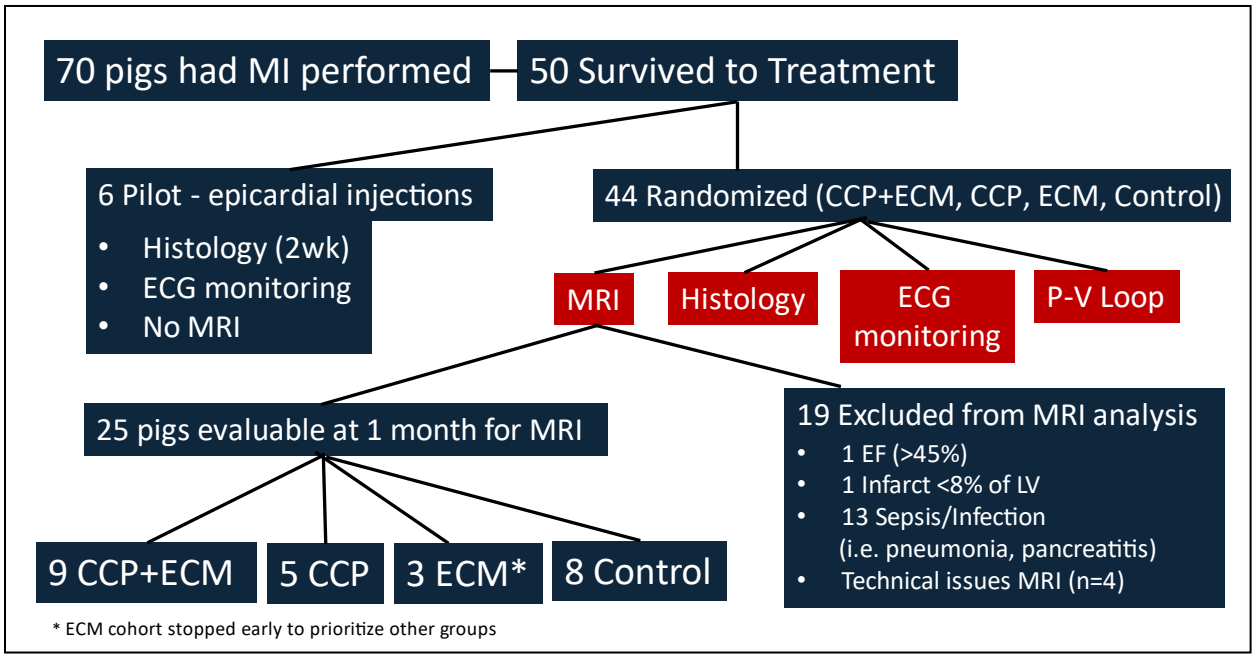

Supplemental Figure 1. Allocation of pigs. Flowchart showing pig allocation following the MI to an initial pilot feasibility cohort and to the 4-group randomized cohort with reasons for exclusions from the final analysis.

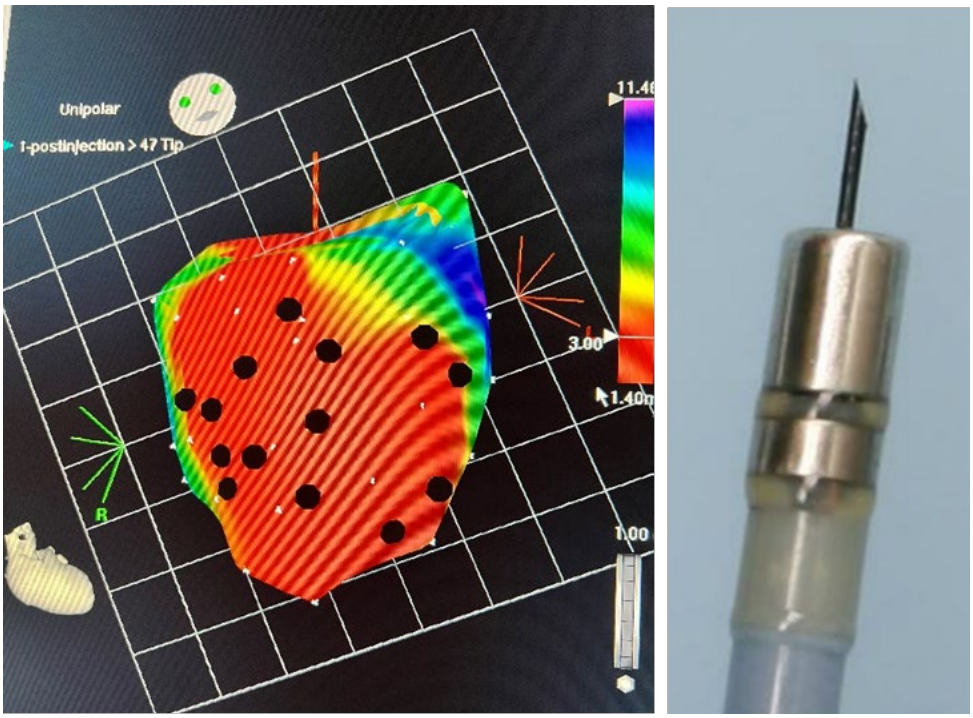

Supplemental Figure 2. (Left image) Representative image of a cardiac unipolar voltage map showing the large infarct zone (red) with 14 annotated injection locations distributed within the infarct and in proximity to the peri-infarct border zone. (Right image) The Myostar, straight needle tipped catheter that is trackable on the electroanatomical mapping system, was used to perform the injections.

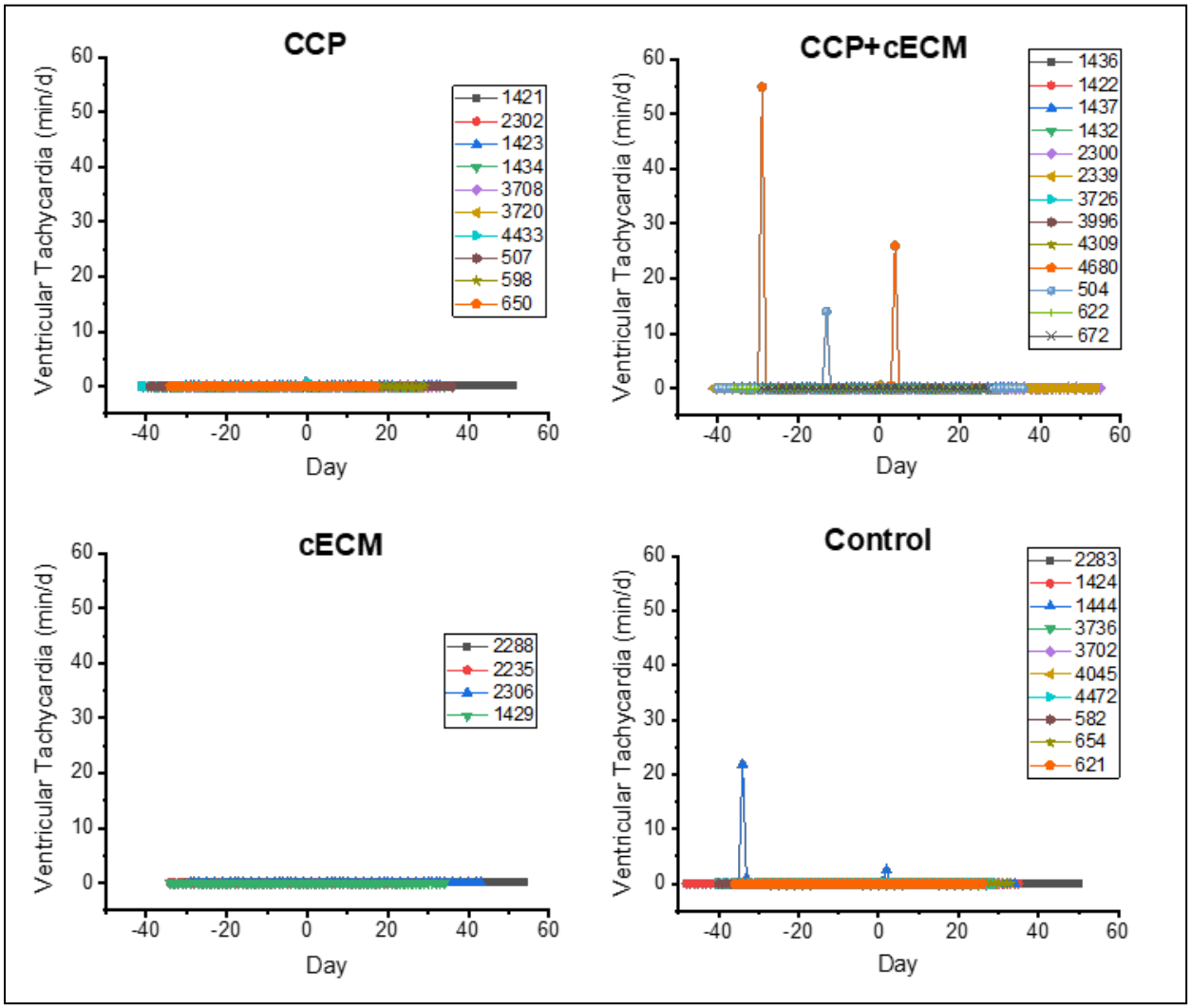

Supplemental Figure 3. **CCP delivery does not result in ventricular tachycardia.** All animals allocated to the 4 groups of the randomized cohort were continuously monitored with implantable loop recorders. The first recordings start the day of the MI surgery and day 0 is the time of transendocardial delivery of the indicated test agent. Plots show the cumulative time the animal is in sustained ventricular tachycardia (defined as >30s) per day. Few animals showed ventricular tachycardia following MI. No animals in the CCP alone group had ventricular tachycardia, and one animal after receiving CCP+cECM had ventricular tachycardia after agent delivery, but this animal also exhibited ventricular tachycardia prior to CCP+cECM delivery.

CCP = committed cardiac progenitor cells, cECM = cardiac extracellular matrix.

REFERENCES

1. Tsao CW, Aday AW, Almarzooq ZI, Alonso A, Beaton AZ, Bittencourt MS, Boehme AK, Buxton AE, Carson AP, Commodore-Mensah Y, Elkind MSV, Evenson KR, Eze-Nliam C, Ferguson JF, Generoso G, Ho JE, Kalani R, Khan SS, Kissela BM, Knutson KL, Levine DA, Lewis TT, Liu J, Loop MS, Ma J, Mussolino ME, Navaneethan SD, Perak AM, Poudel R, Rezk-Hanna M, Roth GA, Schroeder EB, Shah SH, Thacker EL, VanWagner LB, Virani SS, Voecks JH, Wang NY, Yaffe K and Martin SS. Heart Disease and Stroke Statistics-2022 Update: A Report From the American Heart Association. *Circulation*. 2022;145:e153-e639.

2. Rana JS, Khan SS, Lloyd-Jones DM and Sidney S. Changes in Mortality in Top 10 Causes of Death from 2011 to 2018. *J Gen Intern Med*. 2021;36:2517-2518.

3. Zhang J, Bolli R, Garry DJ, Marban E, Menasche P, Zimmermann WH, Kamp TJ, Wu JC and Dzau VJ. Basic and Translational Research in Cardiac Repair and Regeneration: JACC State-of-the-Art Review. *J Am Coll Cardiol*. 2021;78:2092-2105.

4. Riegler J, Tiburcy M, Ebert A, Tzatzalos E, Raaz U, Abilez OJ, Shen Q, Kooreman NG, Neofytou E, Chen VC, Wang M, Meyer T, Tsao PS, Connolly AJ, Couture LA, Gold JD, Zimmermann WH and Wu JC. Human Engineered Heart Muscles Engraft and Survive Long Term in a Rodent Myocardial Infarction Model. *Circ Res*. 2015;117:720-30.

5. Laflamme MA, Chen KY, Naumova AV, Muskheli V, Fugate JA, Dupras SK, Reinecke H, Xu C, Hassanipour M, Police S, O'Sullivan C, Collins L, Chen Y, Minami E, Gill EA, Ueno S, Yuan C, Gold J and Murry CE. Cardiomyocytes derived from human embryonic stem cells in pro-survival factors enhance function of infarcted rat hearts. *Nat Biotechnol*. 2007;25:1015-24.

6. Caspi O, Huber I, Kehat I, Habib M, Arbel G, Gepstein A, Yankelson L, Aronson D, Beyar R and Gepstein L. Transplantation of human embryonic stem cell-derived cardiomyocytes improves myocardial performance in infarcted rat hearts. *J Am Coll Cardiol*. 2007;50:1884-93.

7. Weinberger F, Breckwoldt K, Pecha S, Kelly A, Geertz B, Starbatty J, Yorgan T, Cheng KH, Lessmann K, Stolen T, Scherrer-Crosbie M, Smith G, Reichenspurner H, Hansen A and Eschenhagen T. Cardiac repair in guinea pigs with human engineered heart tissue from induced pluripotent stem cells. *Sci Transl Med*. 2016;8:363ra148.

8. Shiba Y, Fernandes S, Zhu WZ, Filice D, Muskheli V, Kim J, Palpant NJ, Gantz J, Moyes KW, Reinecke H, Van Biber B, Dardas T, Mignone JL, Izawa A, Hanna R, Viswanathan M, Gold JD, Kotlikoff MI, Sarvazyan N, Kay MW, Murry CE and Laflamme MA. Human ES-cell-derived cardiomyocytes electrically couple and suppress arrhythmias in injured hearts. *Nature*. 2012;489:322-5.

9. Dhahri W, Sadikov Valdman T, Wilkinson D, Pereira E, Ceylan E, Andharia N, Qiang B, Masoudpour H, Wulkan F, Quesnel E, Jiang W, Funakoshi S, Mazine A, Gomez-Garcia MJ, Latifi N, Jiang Y, Huszti E, Simmons CA, Keller G and Laflamme MA. In Vitro Matured Human Pluripotent Stem Cell-Derived Cardiomyocytes Form Grafts With Enhanced Structure and Function in Injured Hearts. *Circulation*. 2022;145:1412-1426.

10. Romagnuolo R, Masoudpour H, Porta-Sanchez A, Qiang B, Barry J, Laskary A, Qi X, Masse S, Magtibay K, Kawajiri H, Wu J, Valdman Sadikov T, Rothberg J, Panchalingam KM, Titus E, Li RK, Zandstra PW, Wright GA, Nanthakumar K, Ghugre NR, Keller G and Laflamme MA. Human Embryonic Stem Cell-Derived Cardiomyocytes Regenerate the Infarcted Pig Heart but Induce Ventricular Tachyarrhythmias. *Stem cell reports*. 2019;12:967-981.

11. Zhao M, Nakada Y, Wei Y, Bian W, Chu Y, Borovjagin AV, Xie M, Zhu W, Nguyen T, Zhou Y, Serpooshan V, Walcott GP and Zhang J. Cyclin D2 Overexpression Enhances the Efficacy of Human Induced Pluripotent Stem Cell-Derived Cardiomyocytes for Myocardial Repair in a Swine Model of Myocardial Infarction. *Circulation*. 2021;144:210-228.

12. Chong JJ, Yang X, Don CW, Minami E, Liu YW, Weyers JJ, Mahoney WM, Van Biber B, Cook SM, Palpant NJ, Gantz JA, Fugate JA, Muskheli V, Gough GM, Vogel KW, Astley CA, Hotchkiss CE, Baldessari A, Pabon L, Reinecke H, Gill EA, Nelson V, Kiem HP, Laflamme MA and Murry CE. Human embryonic-stem-cell-derived cardiomyocytes regenerate non-human primate hearts. *Nature*. 2014;510:273-7.

13. Liu YW, Chen B, Yang X, Fugate JA, Kalucki FA, Futakuchi-Tsuchida A, Couture L, Vogel KW, Astley CA, Baldessari A, Ogle J, Don CW, Steinberg ZL, Seslar SP, Tuck SA, Tsuchida H, Naumova AV, Dupras SK, Lyu MS, Lee J, Hailey DW, Reinecke H, Pabon L, Fryer BH, MacLellan WR, Thies RS and Murry CE. Human embryonic stem cell-derived cardiomyocytes restore function in infarcted hearts of non-human primates. *Nat Biotechnol*. 2018;36:597-605.

14. Shiba Y, Gomibuchi T, Seto T, Wada Y, Ichimura H, Tanaka Y, Ogasawara T, Okada K, Shiba N, Sakamoto K, Ido D, Shiina T, Ohkura M, Nakai J, Uno N, Kazuki Y, Oshimura M, Minami I and Ikeda U. Allogeneic transplantation of iPS cell-derived cardiomyocytes regenerates primate hearts. *Nature*. 2016;538:388-391.

15. Menasche P, Vanneaux V, Hagege A, Bel A, Cholley B, Parouchev A, Cacciapuoti I, Al-Daccak R, Benhamouda N, Blons H, Agbulut O, Tosca L, Trouvin JH, Fabreguettes JR, Bellamy V, Charron D, Tartour E, Tachdjian G, Desnos M and Larghero J. Transplantation of Human Embryonic Stem Cell-Derived Cardiovascular Progenitors for Severe Ischemic Left Ventricular Dysfunction. *J Am Coll Cardiol*. 2018;71:429-438.

16. Yap L, Chong LY, Tan C, Adusumalli S, Seow M, Guo J, Cai Z, Loo SJ, Lim E, Tan RS, Grishina E, Soong PL, Lath N, Ye L, Petretto E and Tryggvason K. Pluripotent stem cell-derived committed cardiac progenitors remuscularize damaged ischemic hearts and improve their function in pigs. *NPJ Regen Med*. 2023;8:26.

17. Schmuck EG, Roy S, Dhillon A, Walker S, Spinali K, Colevas S, Zhou T, Chhabra G, Liu Y, Kader Sagar MA, Childs CJ, Kink JA, Eliceiri KW, Hematti P and Raval AN. Cultured cardiac fibroblasts and myofibroblasts express Sushi Containing Domain 2 and assemble a unique fibronectin rich matrix. *Exp Cell Res*. 2021;399:112489.

18. Roy S, Spinali K, Schmuck EG, Kink JA, Hematti P and Raval AN. Cardiac fibroblast derived matrix-educated macrophages express VEGF and IL-6, and recruit mesenchymal stromal cells. *J Immunol Regen Med*. 2020;10.

19. Schmuck EG, Mulligan JD, Ertel RL, Kouris NA, Ogle BM, Raval AN and Saupe KW. Cardiac fibroblast-derived 3D extracellular matrix seeded with mesenchymal stem cells as a novel device to transfer cells to the ischemic myocardium. *Cardiovascular engineering and technology*. 2014;5:119-131.

20. Schmuck EG, Hacker TA, Schreier DA, Chesler NC and Wang Z. Beneficial effects of mesenchymal stem cell delivery via a novel cardiac bioscaffold on right ventricles of pulmonary arterial hypertensive rats. *Am J Physiol Heart Circ Physiol*. 2019;316:H1005-H1013.

21. Schmuck EG, Koch JM, Hacker TA, Hatt CR, Tomkowiak MT, Vigen KK, Hendren N, Leitzke C, Zhao YQ, Li Z, Centanni JM, Hei DJ, Schwahn D, Kim J, Hematti P and Raval AN. Intravenous Followed by X-ray Fused with MRI-Guided Transendocardial Mesenchymal Stem Cell Injection Improves Contractility Reserve in a Swine Model of Myocardial Infarction. *J Cardiovasc Transl Res*. 2015;8:438-48.

22. Tomkowiak MT, Klein AJ, Vigen KK, Hacker TA, Speidel MA, VanLysel MS and Raval AN. Targeted transendocardial therapeutic delivery guided by MRI-x-ray image fusion. *Catheter Cardiovasc Interv*. 2011;78:468-78.

23. Kornowski R, Fuchs S, Tio FO, Pierre A, Epstein SE and Leon MB. Evaluation of the acute and chronic safety of the biosense injection catheter system in porcine hearts. *Catheter Cardiovasc Interv*. 1999;48:447-53; discussion 454-5.

24. Gepstein L, Hayam G and Ben-Haim SA. A novel method for nonfluoroscopic catheter-based electroanatomical mapping of the heart. In vitro and in vivo accuracy results. *Circulation*. 1997;95:1611-22.

25. Ben-Haim SA, Osadchy D, Schuster I, Gepstein L, Hayam G and Josephson ME. Nonfluoroscopic, in vivo navigation and mapping technology. *Nat Med*. 1996;2:1393-5.

26. Evseenko D, Zhu Y, Schenke-Layland K, Kuo J, Latour B, Ge S, Scholes J, Dravid G, Li X, MacLellan WR and Crooks GM. Mapping the first stages of mesoderm commitment during differentiation of human embryonic stem cells. *Proc Natl Acad Sci U S A*. 2010;107:13742-7.

27. Kattman SJ, Witty AD, Gagliardi M, Dubois NC, Niapour M, Hotta A, Ellis J and Keller G. Stage-specific optimization of activin/nodal and BMP signaling promotes cardiac differentiation of mouse and human pluripotent stem cell lines. *Cell Stem Cell*. 2011;8:228-40.

28. Zhang J, Tao R, Campbell KF, Carvalho JL, Ruiz EC, Kim GC, Schmuck EG, Raval AN, da Rocha AM, Herron TJ, Jalife J, Thomson JA and Kamp TJ. Functional cardiac fibroblasts derived from human pluripotent stem cells via second heart field progenitors. *Nature communications*. 2019;10:2238.

29. Sultana N, Zhang L, Yan J, Chen J, Cai W, Razzaque S, Jeong D, Sheng W, Bu L, Xu M, Huang GY, Hajjar RJ, Zhou B, Moon A and Cai CL. Resident c-kit(+) cells in the heart are not cardiac stem cells. *Nature communications*. 2015;6:8701.

30. van Berlo JH, Kanisicak O, Maillet M, Vagnozzi RJ, Karch J, Lin SC, Middleton RC, Marban E and Molkentin JD. c-kit+ cells minimally contribute cardiomyocytes to the heart. *Nature*. 2014;509:337-41.

31. Song H, Yoon C, Kattman SJ, Dengler J, Masse S, Thavaratnam T, Gewarges M, Nanthakumar K, Rubart M, Keller GM, Radisic M and Zandstra PW. Interrogating functional integration between injected pluripotent stem cell-derived cells and surrogate cardiac tissue. *Proc Natl Acad Sci U S A*. 2010;107:3329-34.

32. Fernandes S, Chong JJH, Paige SL, Iwata M, Torok-Storb B, Keller G, Reinecke H and Murry CE. Comparison of Human Embryonic Stem Cell-Derived Cardiomyocytes, Cardiovascular Progenitors, and Bone Marrow Mononuclear Cells for Cardiac Repair. *Stem cell reports*. 2015;5:753-762.

33. Blin G, Nury D, Stefanovic S, Neri T, Guillevic O, Brinon B, Bellamy V, Rucker-Martin C, Barbry P, Bel A, Bruneval P, Cowan C, Pouly J, Mitalipov S, Gouadon E, Binder P, Hagege A, Desnos M, Renaud JF, Menasche P and Puceat M. A purified population of multipotent cardiovascular progenitors derived from primate pluripotent stem cells engrafts in postmyocardial infarcted nonhuman primates. *J Clin Invest*. 2010;120:1125-39.

34. Zhu K, Wu Q, Ni C, Zhang P, Zhong Z, Wu Y, Wang Y, Xu Y, Kong M, Cheng H, Tao Z, Yang Q, Liang H, Jiang Y, Li Q, Zhao J, Huang J, Zhang F, Chen Q, Li Y, Chen J, Zhu W, Yu H, Zhang J, Yang HT, Hu X and Wang J. Lack of Remuscularization Following Transplantation of Human Embryonic Stem Cell-Derived Cardiovascular Progenitor Cells in Infarcted Nonhuman Primates. *Circ Res*. 2018;122:958-969.

35. Poch CM, Foo KS, De Angelis MT, Jennbacken K, Santamaria G, Bahr A, Wang QD, Reiter F, Hornaschewitz N, Zawada D, Bozoglu T, My I, Meier A, Dorn T, Hege S, Lehtinen ML, Tsoi YL, Hovdal D, Hyllner J, Schwarz S, Sudhop S, Jurisch V, Sini M, Fellows MD, Cummings M, Clarke J, Baptista R, Eroglu E, Wolf E, Klymiuk N, Lu K, Tomasi R, Dendorfer A, Gaspari M, Parrotta E, Cuda G, Krane M, Sinnecker D, Hoppmann P, Kupatt C, Fritsche-Danielson R, Moretti A, Chien KR and Laugwitz KL. Migratory and anti-fibrotic programmes define the regenerative potential of human cardiac progenitors. *Nature cell biology*. 2022;24:659-671.

36. Nakamura K, Neidig LE, Yang X, Weber GJ, El-Nachef D, Tsuchida H, Dupras S, Kalucki FA, Jayabalu A, Futakuchi-Tsuchida A, Nakamura DS, Marchiano S, Bertero A, Robinson MR, Cain K, Whittington D, Tian R, Reinecke H, Pabon L, Knollmann BC, Kattman S, Thies RS, MacLellan WR and Murry CE. Pharmacologic therapy for engraftment arrhythmia induced by transplantation of human cardiomyocytes. *Stem cell reports*. 2021;16:2473-2487.

37. Kawaguchi S, Soma Y, Nakajima K, Kanazawa H, Tohyama S, Tabei R, Hirano A, Handa N, Yamada Y, Okuda S, Hishikawa S, Teratani T, Kunita S, Kishino Y, Okada M, Tanosaki S, Someya S, Morita Y, Tani H, Kawai Y, Yamazaki M, Ito A, Shibata R, Murohara T, Tabata Y, Kobayashi E, Shimizu H, Fukuda K and Fujita J. Intramyocardial Transplantation of Human iPS Cell-Derived Cardiac Spheroids Improves Cardiac Function in Heart Failure Animals. *JACC Basic Transl Sci*. 2021;6:239-254.

38. Raval AN and Pepine CJ. Clinical Safety Profile of Transendocardial Catheter Injection Systems: A Plea for Uniform Reporting. *Cardiovasc Revasc Med*. 2021;22:100-108.

39. Raval AN, Cook TD, Duckers HJ, Johnston PV, Traverse JH, Abraham WT, Altman PA and Pepine CJ. The CardiAMP Heart Failure trial: A randomized controlled pivotal trial of high-dose autologous bone marrow mononuclear cells using the CardiAMP cell therapy system in patients with post-myocardial infarction heart failure: Trial rationale and study design. *Am Heart J*. 2018;201:141-148.

40. Raval AN, Johnston PV, Duckers HJ, Cook TD, Traverse JH, Altman PA, Dhingra R, Hematti P, Borrello I, Anderson RD and Pepine CJ. Point of care, bone marrow mononuclear cell therapy in ischemic heart failure patients personalized for cell potency: 12-month feasibility results from CardiAMP heart failure roll-in cohort. *Int J Cardiol*. 2021;326:131-138.

41. Cheng YC, Hsieh ML, Lin CJ, Chang CMC, Huang CY, Puntney R, Wu Moy A, Ting CY, Herr Chan DZ, Nicholson MW, Lin PJ, Chen HC, Kim GC, Zhang J, Coonen J, Basu P, Simmons HA, Liu YW, Hacker TA, Kamp TJ and Hsieh PCH. Combined Treatment of Human Induced Pluripotent Stem Cell-Derived Cardiomyocytes and Endothelial Cells Regenerate the Infarcted Heart in Mice and Non-Human Primates. *Circulation*. 2023;148:1395-1409.

42. Zhang H, Xue Y, Pan T, Zhu X, Chong H, Xu C, Fan F, Cao H, Zhang B, Pan J, Zhou Q, Yang G, Wang J and Wang DJ. Epicardial injection of allogeneic human-induced-pluripotent stem cell-derived cardiomyocytes in patients with advanced heart failure: protocol for a phase I/IIa dose-escalation clinical trial. *BMJ Open*. 2022;12:e056264.